DESIGN AND SIMULATION OF A COMBINED SEED AGITATION PLATE FOR AN AIR-SUCTION PRECISION SEED METERING DEVICE WITH MULTIPLE-SEED-PER-HILL BASED ON DEM

/

基于离散元的一穴多粒气吸式精密排种器组合型搅种盘设计与仿真

Zhiwei WANG[1], Deyi ZHANG[1], Sugirbay ADILET[2], Naishuo WEI[1], Yanwu JIANG[1], Jianguo ZHOU[1], Jun CHEN[1*]

[1] College of Mechanical and Electronic Engineering, Northwest A&F University, Yangling, Shaanxi, 712100, China

[2] Research School of Veterinary Medicine and Agriculture, Shakarim University, Semey 071400, Kazakhstan

**Corresponding author: Jun Chen. E-mail address: chenjun_jdxy@nwsuaf.edu.cn*

DOI: https://doi.org/10.35633/inmateh-79-01

***Keywords:** Small-seeded crops, Seed filling, Particle mobility, Multi-sphere modelling, Response surface methodology (RSM), Bench validation*

ABSTRACT

To improve the seed-filling performance of pneumatic precision seed metering devices for small-seeded crops, a U-shaped seed agitation plate and a combined-type agitation plate were developed. The agitation performance of cylindrical, U-shaped, and combined-type agitation plates was evaluated using the average and maximum velocities of the seed population as quantitative indicators. A three-factor, three-level simulation experiment based on the Discrete Element Method (DEM) was conducted, with agitation plate type, rotational speed, and knob height as the main factors. The optimal parameter combinations were determined as follows: for millet, a combined-type agitation plate with a rotational speed of 24.85 r/min and a knob height of 8.36 mm; for broomcorn millet, 24.17 r/min and 7.96 mm; and for rapeseed, 22.93 r/min and 8.57 mm. Bench experiments were carried out to validate the optimized combined-type agitation plate. The seed-filling rates reached 99.3%, 100%, and 99.7% for millet, broomcorn millet, and rapeseed, respectively. The results indicate that the combined-type agitation plate significantly improves seed mobility and filling performance, providing an effective solution for precision seeding of small-seeded crops.

摘要

针对小籽粒气吸式排种器搅种效果不佳而使得排种盘充种效果差的问题，本研究设计了一种U型搅种钮和组合型搅种钮。为了对比和验证圆柱型、U 型、组合型三种搅种盘的搅种质量，以种群在搅种过程中的平均速度和最大速度为评价指标，选取搅种盘类型、搅种盘转速、搅种钮高度为试验因素利用EDEM离散元仿真软件对其进行了三因素三水平正交仿真试验，得到了谷子最佳参数组合为组合型搅种盘、作业速度24.85r/min、搅种钮高度8.36 mm，糜子最佳参数组合为组合型搅种盘、作业速度24.17 r/min、搅种钮高度7.96mm，油菜籽最佳参数组合为组合型搅种盘、作业速度22.93 r/min、搅种钮高度8.57 mm。通过台架试验对谷子，糜子，油菜籽种群搅种钮高度分别为8.4 mm、8.0 mm、8.6 mm时在最低工作速度10r/min时的搅种效果进行验证，组合型搅种盘对应三类种子的充种率分别为99.3%、100%和99.7%，优于圆柱形和U型搅种盘。试验证明组合型搅种盘具有良好的搅种效果，能够满足小籽粒种子的搅种需求。

INTRODUCTION

Millet, broomcorn millet, and rapeseed are important grain and economic crops in Northwest China. Due to the region's arid climate, limited precipitation, and relatively low temperatures, plastic film mulching is widely adopted in crop production *(Bai et al., 2025)*. In addition, because of the low emergence rate of small-seeded crops, hill-drop sowing with multiple seeds per hole is commonly used *(Tan et al., 2025)*.

To improve the seeding quality and efficiency of small seeds, pneumatic precision seed metering devices capable of multi-grain seeding per hole have been increasingly developed *(Gaikwad et al., 2008; Zhang et al., 2015; Rezaei et al., 2019; Yu et al., 2024)*. However, the small size, low mass, and impurity content of these seeds often result in poor flowability within the seed chamber. This leads to insufficient seed filling or seed leakage at the suction holes of the metering plate, thereby reducing seeding stability. To address this issue, seed agitation devices are introduced to enhance seed flowability and improve seed-filling performance. During operation, agitation knobs interact with seeds through contact, extrusion, and collision, promoting particle mobility within the seed chamber *(Yazgi et al., 2007; Onal et al., 2012; Ibrahim et al., 2018; Wang et al., 2023; Li et al., 2025; Li et al., 2026)*.

Previous studies have proposed various methods to improve seed flowability and filling performance. For example, *Shi et al. (2020)* designed a pneumatic combined-hole precision seed metering device with an integrated agitation mechanism, which enhanced seed filling through shaped holes and guided airflow. *Cong et al. (2014)* developed a dual-purpose pneumatic seed metering device with embedded guiding strips to improve seed distribution. *Ren et al. (2024)* improved seed flowability by arranging curved grooves and shaped holes in a staggered configuration. *Lei et al. (2016)* proposed a cylindrical double-helix agitation device to enhance wheat seed mobility, while *Wang et al. (2019)* designed a wedge-shaped agitation structure to improve seeding accuracy in rice seeders. *Li et al. (2019)* and *Li et al. (2024)* further optimized agitation structures to improve seed filling and reduce seed damage under high-speed conditions. International studies have likewise shown that the operating parameters and auxiliary filling structures of pneumatic seed metering devices strongly affect metering performance and crop adaptability *(Singh et al., 2005; Karayel et al., 2022)*, and a recent review further highlighted the growing importance of coupled numerical and experimental approaches in the development of pneumatic seed-metering devices *(Bustos-Gaytán et al., 2025)*.

Although these studies have demonstrated the importance of agitation devices in improving seed flowability and filling performance, most designs focus on specific crops or operating conditions. Systematic research on universal agitation devices suitable for multiple small-seeded crops remains limited. The novelty of this paper lies in the design of a combined-type agitation plate, the DEM-based mechanistic comparison of three knob configurations, and the parameter optimization of a single structure applicable to three representative small-seeded crops.

Preliminary experiments in this study revealed that, for millet, broomcorn millet, and rapeseed, insufficient agitation leads to seed leakage and blockage of suction holes by impurities. Therefore, a U-shaped and a combined-type seed agitation plate were designed to improve seed flowability and stability. Based on DEM simulations using EDEM, the key factors affecting agitation performance were analyzed. A three-factor, three-level experimental design was then conducted to determine the optimal parameter combination of the agitation plate. The results provide a theoretical and technical basis for the design of universal pneumatic precision seed metering systems for small-seeded crops.

MATERIAL AND METHODS

Design and working principle of the seed agitation plate

As shown in Fig. 1, three agitation-knob configurations were designed for the seed agitation plate: cylindrical, U-shaped, and combined types (a combination of cylindrical and U-shaped structures). The agitation plate was designed to be positioned close to the circumferential region of the suction holes on the seed metering plate, while avoiding interference with the seed-cleaning mechanism. In addition, the height of the agitation knobs was optimized to ensure effective seed disturbance without interfering with surrounding components such as the seed chamber housing.

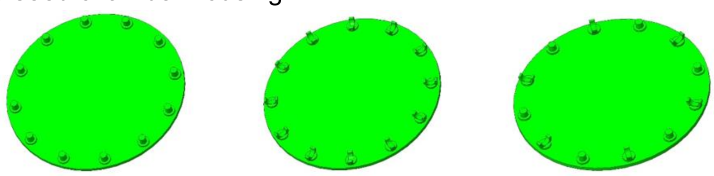

(a) (b) (c)

Fig. 1 - Agitation-knob configurations of the seed agitation plate

(a) Cylindrical type; (b) U-shaped type; (c) Combined type

As shown in Fig. 2, the geometric parameters of the seed agitation plate and agitation knobs are illustrated. To ensure effective interaction between the agitation knobs and the seed population, while maintaining sufficient clearance for the seed-cleaning mechanism, the diameter of the agitation plate (D) and the spacing between symmetrically arranged knobs (d_1) were designed according to the dimensions of the seed metering plate. Simulation-based pre-experiments demonstrated that many factors have negligible effects on the seed-agitating performance. Therefore, considering the matching compatibility with the seed metering plate, the parameters were set as follows: D = 160 mm, d_1 = 140 mm, h_{12} = 2 mm, k_{12} = 10 mm, k_{21} = 3 mm, and d_2 = 10 mm.

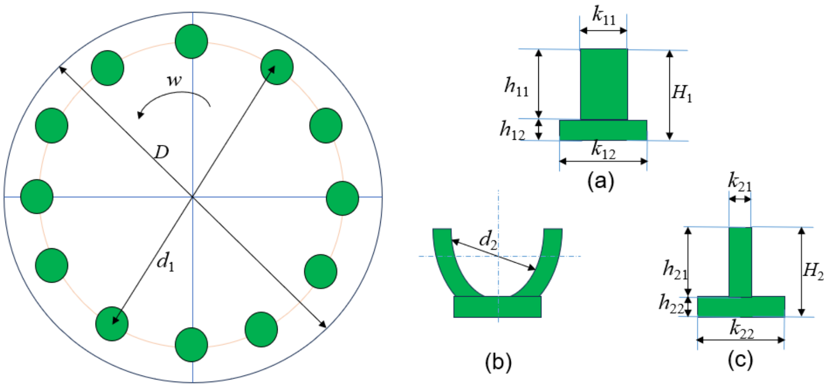

Fig. 2 - Geometric configuration of the seed agitation

(a) Front view of cylindrical type; (b) Front view of U-shaped type; (c) Front view of combined type

A pedestal structure was first introduced on the metering plate, on which the cylindrical and U-shaped agitation knobs were mounted. The number and arrangement of the knobs were determined based on uniform circumferential distribution and sufficient interaction coverage with the seed population. In this study, twelve agitation knobs were evenly distributed along the circumference of the agitation plate.

Considering key factors such as knob geometry, rotational speed of the metering plate, and knob height, the agitation performance was further analyzed using DEM simulations.

DEM-based simulation and analysis of the seed agitation process

Seed particle modeling

Statistical analysis indicated low variability among the effective seed samples. Therefore, one representative seed from each type (millet, broomcorn millet, and rapeseed) was selected for three-dimensional (3D) reconstruction.

Each selected seed was scanned using a portable 3D scanner (EinScan, accuracy ≤ 0.02 mm, Shenzhen Xinlin 3D Co., Ltd., China) to obtain its geometric morphology. The scanned data were processed in VxElements software, including calibration, alignment, mesh generation, and surface reconstruction. The resulting 3D models were exported in STL format.

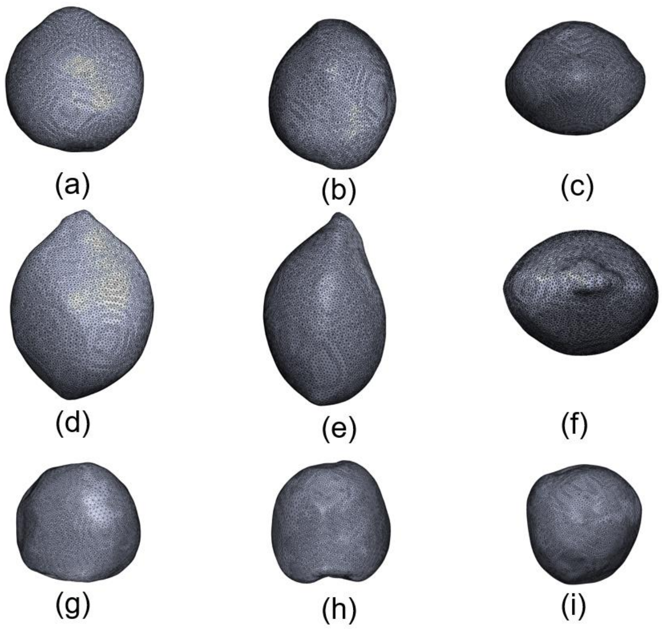

Fig. 3 - 3D reconstructed models of seeds

(a–c) Millet; (d–f) Broomcorn millet; (g–i) Rapeseed

The STL models were subsequently imported into SolidWorks 2021 for visualization, and the corresponding views of the three seed types are shown in Fig. 3.

For DEM simulation in EDEM, the Hertz–Mindlin (no-slip) contact model was used in this simulation, the seed particles were constructed using a multi-sphere approximation method based on the scanned 3D geometries. The millet, broomcorn millet, and rapeseed models were composed of six, eight, and seven spheres, respectively, to balance computational efficiency and shape accuracy.

Because the effective seed samples exhibited relatively small dimensional variation, one representative seed from each crop was used to establish the multi-sphere model. This strategy is suitable for comparative analysis of knob configuration and operating parameters, but it cannot fully represent seed-size dispersion, broken seeds, or impurity particles in real seed lots. Therefore, the present DEM model should be regarded as a simplified but representative model, and its engineering validity was further checked through bench experiments.

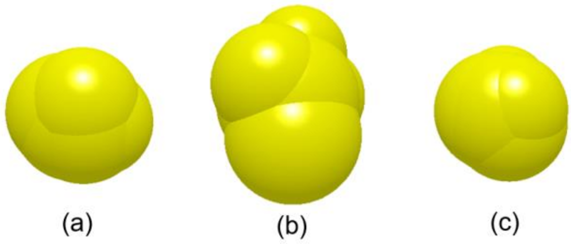

Fig. 4 - Multi-sphere particle models used in EDEM

(a) Millet; (b) Broomcorn millet; (c) Rapeseed

The material and contact parameters used in the simulation were defined based on experimental measurements and literature values *(Yazgi et al., 2007; Onal et al., 2012; Ibrahim et al., 2018; Cui et al., 2025; He et al., 2025; Wang et al., 2025; Zhang et al., 2025)*, as summarized in Table 1.

Table 1

The mechanics parameters of different parts

Item	Value （millet, broomcorn millet, and rapeseed）
Poisson's ratio of seeds	0.27/0.33/0.29
Shear modulus of seeds [Pa]	（1.4/2.6/0.53）×10^8
Seed density [kg/m³]	1015.6/907.7/1132.5
Coefficient of restitution (seed–metering plate)	0.37/0.35/0.41
Dynamic friction coefficient (seed–metering plate)	0.015/0.019/0.017
Static friction coefficient (seed–metering plate)	0.481/0.317/0.387
Coefficient of restitution (seed–agitation knob)	0.35/0.30/0.33
Dynamic friction coefficient (seed–agitation knob)	0.009/0.006/0.011
Static friction coefficient (seed–agitation knob)	0.406/0.331/0.371
Coefficient of restitution (seed–seed)	0.23/0.21/0.27
Dynamic friction coefficient (seed–seed)	0.022/0.015/0.019
Static friction coefficient (seed–seed)	0.46/0.38/0.41
Coefficient of restitution (seed–housing)	0.37/0.33/0.45
Dynamic friction coefficient (seed–housing)	0.021/0.013/0.019
Static friction coefficient (seed–housing)	0.577/0.467/0.517

Construction of DEM model and simulation setup

The three-dimensional model of the seed metering device was developed in SolidWorks 2021, exported in STL format, and imported into EDEM for simulation. The material properties and contact parameters were assigned according to the values listed in Table 1.

A particle generation region was defined at the seed inlet to simulate seed feeding. The particle generation rate of 10,000 particles/s and the total particle number of 40,000 were determined through preliminary simulation trials to ensure rapid chamber filling, continuous particle coverage in the working region around the agitation plate, and stable response values without excessive computational cost. The initial falling velocity of 2 m/s was assigned to allow the particles generated at the inlet to enter the seed chamber smoothly and to avoid artificial accumulation near the particle factory.

Particle generation lasted for 4 s to complete chamber filling, followed by a settling period of approximately 2 s. When the particle velocity decreased below 0.01 m/s, the seed bed was considered to reach a quasi-static state, after which the rotational simulation was initiated.

The metering plate and agitation plate were then assigned rotational motion. Taking a rotational speed of 20 r/min as an example, the angular velocity was set to 120°/s, with rotation about the central axis of the metering plate. The simulation time step was set to 20% of the Rayleigh time step, and the total simulation time was 3 s so that a sufficiently long stable agitation interval could be captured for statistical analysis.

Post-processing and evaluation indices

In the EDEM post-processing module, the velocity distribution of seed particles was visualized using a color scale, where red indicates high velocity and blue indicates low velocity (Fig. 5). The velocity field reflects the agitation intensity induced by the agitation plate.

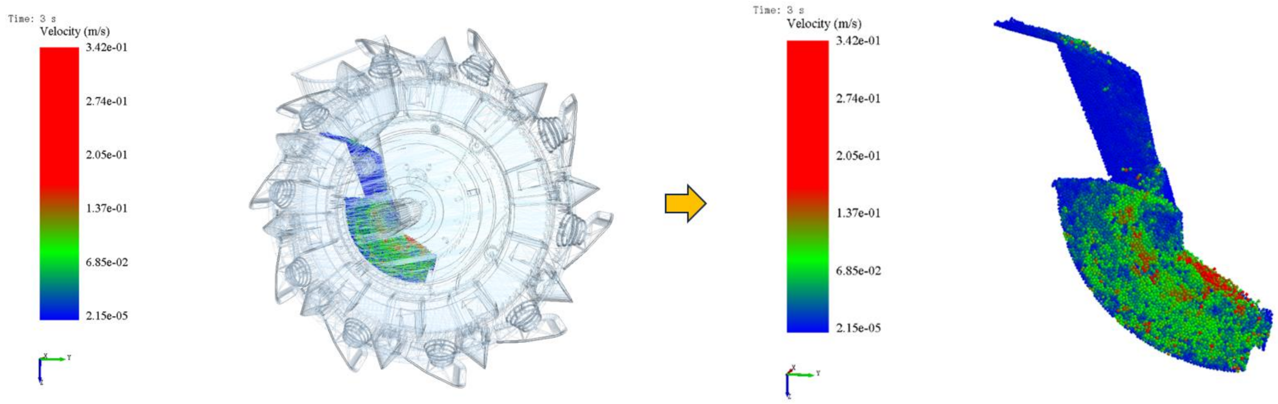

Fig. 5 - Velocity distribution of seed particles during agitation

To quantitatively evaluate the agitation performance, the average velocity and maximum velocity of the seed population were selected as the primary DEM indicators. These two indices reflect the overall particle mobility and the local disturbance intensity in the filling zone, respectively, and are therefore closely related to the seed replenishment capacity near the suction-hole circumferential region. In addition, the seed-filling rate obtained from the bench test was used as an engineering validation index. Because the present DEM model was simplified to facilitate comparative structural optimization, contact frequency and spatial uniformity of particles were not extracted in this study and are discussed as limitations.

Preliminary simulation results

As shown in Fig. 6, the temporal variations of average and maximum velocities for different agitation plate configurations are presented. During the initial stage (0–0.3 s), the velocity curves fluctuate due to startup effects. After 0.3 s, the system reaches a relatively stable state. Therefore, the interval of 0.3–3.0 s was selected for statistical analysis.

Under a rotational speed of 20 r/min and an agitation knob height of 8.0 mm, the average velocities of the seed population for the cylindrical, U-shaped, and combined-type agitation plates were 0.0148 m/s, 0.0153 m/s, and 0.0167 m/s, respectively. The corresponding maximum velocities were 0.3593 m/s, 0.3641 m/s, and 0.4086 m/s.

These results indicate that the geometry and configuration of agitation knobs significantly influence seed agitation performance. The combined-type agitation plate exhibited superior performance compared with the other configurations. Therefore, further analysis considering additional factors is necessary.

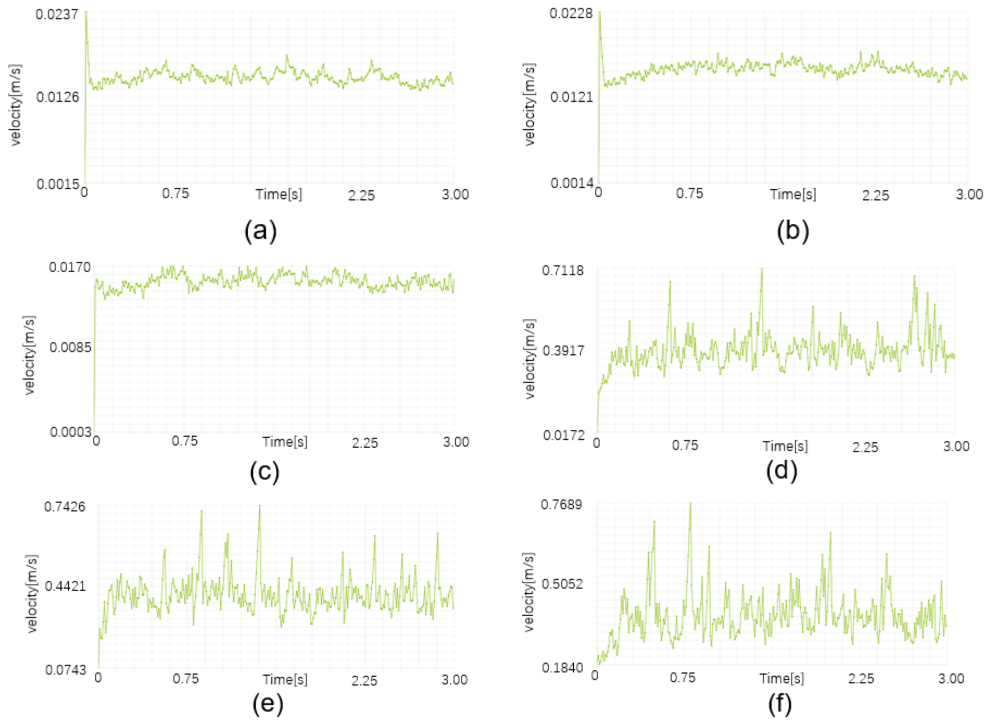

Fig. 6 - Time-dependent velocity curves of seed particles

(a–c) Average velocity each for millet, broomcorn millet, rapeseed;
(d–f) Maximum velocity each for millet, broomcorn millet, rapeseed

Response surface design

Based on the simulation results and preliminary analysis, the agitation knob type, rotational speed of the agitation plate, and agitation knob height were identified as the primary factors influencing seed agitation performance.

Three types of agitation knobs—cylindrical, U-shaped, and combined—were selected as factor X_1. According to the typical operating speed range of seed metering devices (2.0–5.0 km/h), the corresponding rotational speed of the metering plate ranges from 10 to 27 r/min. Therefore, three representative levels (15, 20, and 25 r/min) were selected for factor X_2. Considering the structural constraints and clearance between the agitation knobs and adjacent components (e.g., seed chamber housing and seed-cleaning mechanism), the feasible range of knob height was determined to be 0–15 mm. Accordingly, three levels (6.0, 8.0, and 10.0 mm) were selected for factor X_3 *(Han et al., 2018; Liu et al., 2022; Gao et al., 2023; Ding et al., 2024)*.

A three-factor, three-level response surface design generated in Design-Expert 8.0.6 was adopted, resulting in 17 simulation runs with five center-point replications. Quadratic regression models were then established for the two response variables, and the coded levels of the factors are listed in Table 2.

Table 2

Factor levels used in the experimental design

Code	Agitation knob type (X_1)	Rotational speed (X_2) [r/min]	Agitation knob height (X_3) [mm]
-1	A: Cylindrical	15	6.0
0	B: U-shaped	20	8.0
1	C: Combined	25	10.0

Bench validation of seed-filling performance

Because low rotational speed provides the weakest particle disturbance and therefore the most stringent condition for maintaining seed filling, bench experiments were conducted at the minimum operating condition of the seed metering device (10 r/min, corresponding to a forward speed of 2.0 km/h). Validation under this condition was used to verify whether the optimized structure could still ensure adequate seed replenishment under the least favorable agitation state. The agitation knob height was set according to the optimized simulation results.

However, the present validation was limited to low-speed bench conditions, and further experiments over the full operating-speed range are still required.

The experiments were carried out using a JPS-12 seed metering performance test bench (Heilongjiang Provincial Agricultural Machinery Research Institute, China). The system mainly consists of a seedbed belt, a metering device mounting frame, a hydraulic system, and a high-speed imaging system. The bench has a total length of 9.5 m, a belt width of 0.7 m, and an adjustable forward speed range of 1.5–12.0 km/h. The high-speed camera was operated at 300 frames per second (fps), and the recorded images were processed using i-SPEED Control Software.

Due to the difficulty in directly quantifying seed agitation through visual observation, the seed-filling rate was selected as the engineering validation index of agitation performance. Improved agitation enhances seed mobility in the filling zone, weakens local seed crowding, and reduces the probability of insufficient filling at the suction holes.

For each seed type (millet, broomcorn millet, and rapeseed), corresponding to three different types of seed agitating plates (cylindrical, U-shaped, and combined), 300 consecutive seeding events were recorded for each treatment. The filling and missing conditions of seeds in each hill were captured through a transparent seed chamber using both a high-speed camera and a mobile camera. The average seed-filling rate was calculated based on the recorded data.

(a) (b) (c)

Fig. 7 - Bench validation of seed-filling performance

(a) Millet; (b) Broomcorn millet; (c) Rapeseed

RESULTS AND DISCUSSION

Results and analysis of the experimental design

A three-factor, three-level response surface experiment was conducted using Design-Expert software, resulting in 17 simulation runs. The average velocity (Y_1) and maximum velocity (Y_2) of the seed population were selected as response variables to evaluate agitation performance. The experimental design and corresponding results are summarized in Table 3.

Table 3

Experiment scheme and results

No.	X_1	X_2	X_3	Y_1 [m/s]	Y_2 [m/s]
1	-1	-1	0	0.0152	0.3593
2	1	-1	0	0.0153	0.3651
3	-1	1	0	0.0158	0.3742
4	1	1	0	0.0166	0.4029
5	-1	0	-1	0.0150	0.3621
6	1	0	-1	0.0154	0.3642
7	-1	0	1	0.0152	0.3733
8	1	0	1	0.0161	0.3821
9	0	-1	-1	0.0148	0.3599
10	0	1	-1	0.0153	0.3707
11	0	-1	1	0.0155	0.3642
12	0	1	1	0.0166	0.3964
13	0	0	0	0.0159	0.3848

No.	X_1	X_2	X_3	Y_1 [m/s]	Y_2 [m/s]
14	0	0	0	0.0157	0.3774
15	0	0	0	0.0160	0.3753
16	0	0	0	0.0163	0.3842
17	0	0	0	0.0163	0.3898

Regression modeling and ANOVA

The experimental results were analyzed to obtain polynomial regression equations, in which the average population velocity and the maximum population velocity were taken as the response variables, and the coded values of the factors were used as independent variables, as follows:

$$Y_1 = 0.016 + 0.000275X_1 + 0.0004375X_2 + 0.0003625X_3 + 0.000175X_1X_2 + 0.000125X_1X_3 + 0.00015X_2X_3 - 0.00022X_1^2 - 0.000095X_2^2 - 0.000395X_3^2 \quad (1)$$

$$Y_2 = 0.38 + 0.005675X_1 + 0.012X_2 + 0.007388X_3 + 0.005725X_1X_2 + 0.001675X_1X_3 + 0.00535X_2X_3 - 0.00465X_1^2 - 0.002275X_2^2 - 0.007225X_3^2 \quad (2)$$

Quadratic regression models were developed for both response variables (Y_1 and Y_2) based on the coded factors. Analysis of variance (ANOVA) results (Tables 4 and 5) indicate that both models are statistically significant ($p < 0.05$), with no significant lack-of-fit ($p > 0.05$), confirming the adequacy of the regression models.

Table 4

ANOVA of the seed population average speed Y_1

Sources	Sum of squares	Degree of freedom	Mean square	F	p
Model	4.43×10^{-6}	9	4.93×10^{-7}	7.59	0.0070
X_1	6.05×10^{-7}	1	6.05×10^{-7}	9.32	0.0185
X_2	1.53×10^{-6}	1	1.53×10^{-6}	23.58	0.0018
X_3	1.05×10^{-6}	1	1.05×10^{-6}	16.19	0.0050
X_1X_2	1.2325×10^{-7}	1	1.2325×10^{-7}	1.8867	0.2119
X_1X_3	6.2516×10^{-8}	1	6.2516×10^{-8}	0.9626	0.3592
X_2X_3	9.2145×10^{-8}	1	9.2145×10^{-8}	1.3861	0.2775
X_1^2	2.0403×10^{-7}	1	2.0403×10^{-7}	3.1387	0.1198
X_2^2	3.8624×10^{-8}	1	3.8624×10^{-8}	0.5853	0.4693
X_3^2	6.5746×10^{-7}	1	6.5746×10^{-7}	10.1180	0.0155
Lack of fit	1.83×10^{-7}	3	6.08×10^{-8}	0.89	0.5171
Pure error	2.72×10^{-7}	4	6.81×10^{-8}		
Total	4.89×10^{-6}	16			

Table 5

ANOVA of the seed population maximum speed Y_2

Sources	Sum of squares	Degree of freedom	Mean square	F	p
Model	2.46×10^{-3}	9	2.73×10^{-4}	8.67	0.0047
X_1	2.58×10^{-4}	1	2.58×10^{-4}	8.18	0.0244
X_2	1.15×10^{-3}	1	1.15×10^{-3}	36.33	0.0005
X_3	4.37×10^{-4}	1	4.37×10^{-4}	13.85	0.0074
X_1X_2	1.3112×10^{-4}	1	1.3112×10^{-4}	4.1601	0.0808
X_1X_3	1.1277×10^{-5}	1	1.1277×10^{-5}	0.3561	0.5695
X_2X_3	1.1403×10^{-4}	1	1.1403×10^{-4}	3.6330	0.0983
X_1^2	9.1227×10^{-5}	1	9.1227×10^{-5}	2.8889	0.1330

Sources	Sum of squares	Degree of freedom	Mean square	*F*	*p*
X_2^2	2.1873×10^{-5}	1	2.1873×10^{-5}	0.6915	0.4331
X_3^2	2.2746×10^{-4}	1	2.2746×10^{-4}	6.9743	0.0334
Lack of fit	8.15×10^{-5}	3	2.72×10^{-5}	0.78	0.5632
Pure error	1.39×10^{-4}	4	3.48×10^{-5}		
Total	2.68×10^{-3}	16			

For both response variables, the main factors X_1 (agitation knob type), X_2 (rotational speed), and X_3 (knob height) significantly affected the results ($p < 0.05$), while interaction terms were generally insignificant. The quadratic term X_3^2 also showed a significant effect, indicating a nonlinear relationship between knob height and agitation performance.

Effect of factors on average velocity (Y_1)

The response surfaces for the average velocity are shown in Fig. 8. Among the three factors, rotational speed (X_2) exhibited the most significant influence, followed by knob height (X_3), while knob type (X_1) had a relatively smaller effect.

As the knob configuration changed from cylindrical to U-shaped and then to the combined type, the average velocity of the seed population increased. The cylindrical part mainly breaks the compact seed layer and promotes upward and radial displacement, whereas the U-shaped part provides a temporary guiding and holding space for particles. Their combination extends the particle-structure interaction path, increases the disturbance depth, and reduces the low-mobility region near the chamber wall, thereby improving continuous seed replenishment around the suction-hole zone.

With increasing rotational speed, the average velocity increased monotonically because more kinetic energy was transferred from the rotating structure to the seed population per unit time. In contrast, knob height exhibited a quadratic effect. When the height was too small, the disturbance depth was insufficient and only the superficial seed layer was mobilized. When the height became excessive, particles were overly squeezed toward the chamber wall, leading to local congestion and a reduction in overall particle circulation.

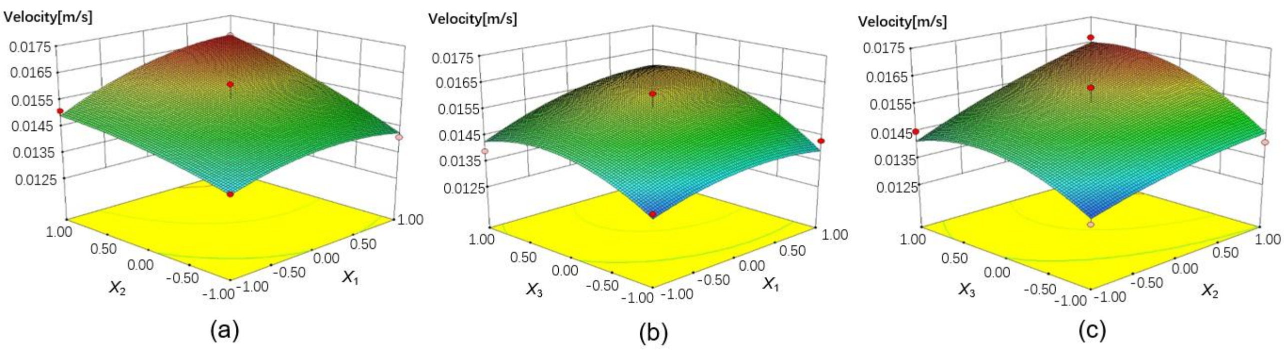

Fig. 8 - Response surfaces to influences of different factors on the seed population average speed

(a) X_1 and X_2; (b) X_1 and X_3; (c) X_2 and X_3

Effect of factors on maximum velocity (Y_2)

The response surfaces for maximum velocity are presented in Fig. 9. Similar trends were observed for Y_2 as for Y_1. Rotational speed remained the most influential factor, followed by knob height, while knob type had the least effect. Compared with the average velocity, the maximum velocity responds more sensitively to local strong interactions between the knob and nearby particles.

Increasing rotational speed significantly enhanced the maximum velocity of seed particles because the instantaneous particle-structure interaction became stronger. The influence of knob height also exhibited a nonlinear effect. An excessively large knob height reduced the free-movement space of particles and converted part of the agitation effect into compressive crowding rather than effective acceleration.

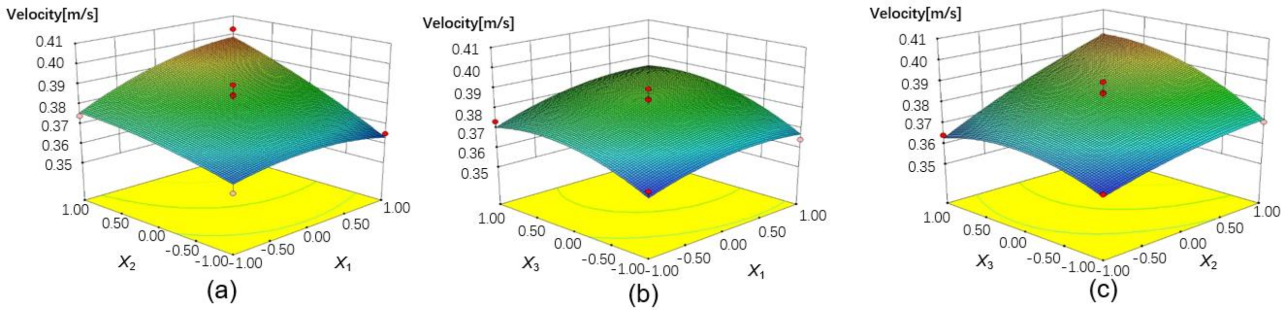

Fig. 9 - Response surfaces to influences of different factors on the seed population maximum speed
(a) X_1 and X_2; (b) X_1 and X_3; (c) X_2 and X_3

The consistent trends observed for both response variables confirm the reliability of the simulation results. From an engineering perspective, the superior performance of the combined-type agitation plate indicates that a moderate increase in particle mobility is beneficial to low-speed seed filling. Because the agitation mechanism is mounted on the existing rotating plate and operates within a relatively low speed range, its additional energy demand is expected to be limited. Moreover, the disturbance mode is dominated by pushing and rolling rather than high-energy impact, so obvious seed damage is not expected. However, direct seed-damage and germination tests were not conducted in this study, and these aspects should be included in future work. The proposed structure can also be extended to other small-seeded crops by re-matching the knob height, chamber clearance, and rotational speed according to seed size and flowability.

Optimization of parameters

Based on the regression models, the optimal parameter combinations were obtained for each seed type. For millet, the optimal configuration was a combined-type agitation plate with a rotational speed of 24.85 r/min and a knob height of 8.36 mm. For broomcorn millet, the optimal parameters were 24.17 r/min and 7.96 mm, while for rapeseed, the optimal values were 22.93 r/min and 8.57 mm.

The results indicate that the combined-type agitation plate consistently provides superior agitation performance across all seed types.

The simulation results demonstrate that agitation performance improves with increasing rotational speed. However, to ensure practical applicability, the optimized design must also perform effectively under low-speed conditions. Therefore, validation experiments were conducted at the minimum operating speed (10 r/min) using the optimized knob heights for each seed type. This choice represents the most unfavorable agitation condition for the device; nevertheless, the present experimental verification is still limited to low-speed bench conditions, and future studies should extend the validation to the full operating-speed range and integrated field conditions.

Bench test validation results

As shown in Fig. 10, the seed-filling performance of the seed holes on the seed plate after the agitation process is presented.

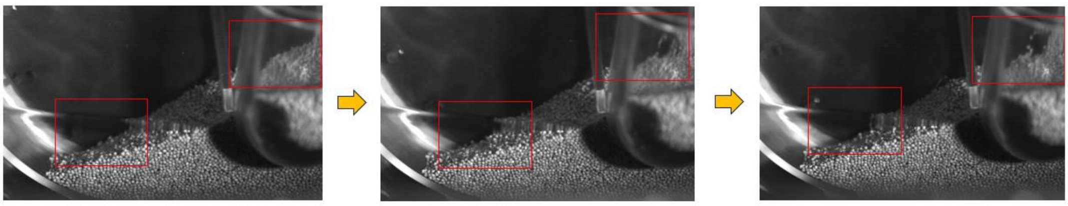

Fig. 10 - Variation of the millet population under the action of the combined agitation plate

The filling condition was analyzed and statistically evaluated on a hole-by-hole basis using recordings from a high-speed camera and a mobile phone. Under the conditions where multiple-seed adsorption was neglected and the seed-cleaning device was not activated, the results indicate that at an operating speed of 10 r/min, for the combined agitation plate, the seed-filling rates of millet, broomcorn millet, and rapeseed were 99.3%, 100%, and 99.7%, respectively; for the cylindrical seed agitation plate, the corresponding seed-filling rates were 94.3%, 97.0%, and 96.3%, respectively; and for the U-shaped seed agitation plate, the corresponding values were 97.3%, 98.7%, and 98.0%, respectively. These results demonstrate that the combined seed agitation plate exhibits superior agitation performance compared with the other two types, thereby satisfying the design requirements of the seed agitation mechanism of the seed metering device.

CONCLUSIONS

This study developed U-shaped and combined-type agitation plates to improve the agitation performance of pneumatic seed metering devices for small-seeded crops. Based on DEM simulations and bench validation experiments, the following conclusions were obtained.

(1) The agitation performance of cylindrical, U-shaped, and combined-type configurations was systematically evaluated using the average and maximum velocities of seed particles as response variables. The combined-type agitation plate exhibited superior performance compared with the other two configurations.

(2) A three-factor, three-level experimental design was conducted to analyze the effects of agitation plate type, rotational speed, and knob height. The optimal parameter combinations were identified as follows: for millet, 24.85 r/min and 8.36 mm; for broomcorn millet, 24.17 r/min and 7.96 mm; and for rapeseed, 22.93 r/min and 8.57 mm, all with the combined-type agitation plate.

(3) Bench validation experiments confirmed that, under the minimum operating speed of 10 r/min, the optimized agitation configurations achieved high seed-filling rates of 99.3%, 100%, and 99.7% for millet, broomcorn millet, and rapeseed, respectively. These results demonstrate that the proposed agitation plate effectively enhances seed-filling performance and meets the operational requirements of precision seeding under the least favorable agitation condition.

The proposed design provides a practical structural option for improving the low-speed filling stability of pneumatic precision seed metering devices for millet, broomcorn millet, and rapeseed. Future studies should incorporate seed-size distributions and impurity particles into the DEM model and carry out seed-damage, germination, full-speed bench, and integrated field validations.

ACKNOWLEDGEMENT

This study was supported by the National Natural Science Foundation of China (32272001), the Shaanxi Key Research and Development Project (2023-ZDLNY-62), and the Shaanxi Key Research and Development Project (grant number 2022NY-205).

REFERENCES

[1] Bai S., Yuan Y., Niu K., Zhou L., Zhao B., & Yu Y. (2025). Design and test of operation quality monitoring system for cotton precision film-laying hole seeder (棉花精量铺膜穴播机作业质量监测系统设计与试验). *Transactions of the Chinese Society for Agricultural Machinery*, 56(5), 49-58. https://doi.org/10.6041/j.issn.1000-1298.2025.05.005

[2] Bustos-Gaytán A., Saldaña-Robles N., Joya-Cárdenas D.R., Gutiérrez-Vaca C., Alfaro-Ayala J.A., Barco-Burgos J., & Saldaña-Robles A. (2025). Advancements in pneumatic seed-metering devices: A review of numerical and experimental approaches. *Results in Engineering*, 26, 105626. https://doi.org/10.1016/j.rineng.2025.105626

[3] Cong J., Liao Q., Cao X., Liao Y., Yu J., & Wang L. (2014). Seed filling performance of dual-purpose seed plate in metering device for both rapeseed & wheat seed (油菜小麦兼用排种盘的排种器充种性能). *Transactions of the Chinese Society of Agricultural Engineering*, 30(8), 30-39. https://doi.org/10.3969/j.issn.1002-6819.2014.08.004

[4] Cui Y., Ye S., Feng S., & Zheng D. (2025). Calibration of discrete element simulation parameters for buckwheat seeds. *INMATEH Agricultural Engineering*, 75(1), 110-120. https://doi.org/10.35633/inmateh-75-09

[5] Ding L., Yuan Y., Dou Y., Li C., He Z., Guo G., Zhang Y., Chen B., & Li H. (2024). Design and experiment of air-suction maize seed-metering device with auxiliary guide. *Agriculture*, 14(2), 169. https://doi.org/10.3390/agriculture14020169

[6] Gaikwad B.B., & Sirohi N.P.S. (2008). Design of a low-cost pneumatic seeder for nursery plug trays. Biosystems Engineering, 99(3), 322-329. https://doi.org/10.1016/j.biosystemseng.2007.10.017

[7] Gao X., Xie G., Li J., Shi G., Lai Q., & Huang Y. (2023). Design and validation of a centrifugal variable-diameter pneumatic high-speed precision seed-metering device for maize. *Biosystems Engineering*, 227, 161-181. https://doi.org/10.1016/j.biosystemseng.2023.02.004

[8] Han D., Zhang D., Jing H., Yang L., Cui T., Ding Y., Wang Z., Wang Y., & Zhang T. (2018). DEM-CFD coupling simulation and optimization of an inside-filling air-blowing maize precision see

d-metering device. *Computers and Electronics in Agriculture*, 150, 426-438. https://doi.org/10.1016/j.compag.2018.05.006

[9] He Y., Ji X., Dun G., Liu X., Mu A., & Ma, C. (2025). Discrete element simulation calibration of contact parameters for millet seeds. *INMATEH Agricultural Engineering*, 76(2), 686-696. https://doi.org/10.35633/inmateh-76-58

[10] Ibrahim, E. J., Liao, Q., Wang, L., Liao, Y., & Yao, L. (2018). Design and experiment of multi-row pneumatic precision metering device for rapeseed. *International Journal of Agricultural and Biological Engineering*, 11(5), 116-123. https://doi.org/10.25165/j.ijabe.20181105.3544

[11] Karayel D., Barut Z.B., & Özmerzi A. (2022). Estimation of optimum vacuum pressure of air-suction seed-metering device of precision seeders using artificial neural network models. *Agronomy*, 12(7), 1600. https://doi.org/10.3390/agronomy12071600

[12] Lei X., Liao Y., Li Z., Zhang W., Li S., & Liao Q. (2016). Design of seed churning device in air-assisted centralized metering device for rapeseed and wheat and experiment on seed filling performance (油菜小麦兼用气送式集排器搅种装置设计及充种性能试验). *Transactions of the Chinese Society of Agricultural Engineering*, 32(18), 26-34. https://doi.org/10.11975/j.issn.1002-6819.2016.18.004

[13] Li H., Yang Li, Zhang D., Cui T., He X., & Li Z. (2026). Seed motion and force characteristics in pneumatic seed delivery device based on CFD-DEM coupling (基于 CFD-DEM 耦合的气力式导种装置中种子运动与受力研究). *Transactions of the Chinese Society for Agricultural Machinery*, 57(6), 104-118. https://doi.org/10.6041/j.issn.1000-1298.2026.06.010

[14] Li X., Liao Q., Du W., Wang X., Liao Y., & Yuan J. (2024). Damage patterns and germination experiments of rice seeds using high-speed air-assisted centralized seed metering device (高速气送集排器水稻种子损伤规律及发芽试验). *Transactions of the Chinese Society of Agricultural Engineering*, 40(21), 46-55. https://doi.org/10.11975/j.issn.1002-6819.202406072

[15] Li Z., An S., Yang Li, Zhang D., He X., & Cui T. (2025). Analysis and structural optimization of filling and releasing mechanism for pneumatic high-speed precision maize seed-metering device. *Transactions of the CSAM*, 56(9), 62-72，128. https://doi.org/10.6041/j.issn.1000-1298.2025.09.005

[16] Li Z., Yang W., Zhang T., Wang W., Zhang S., & Chen L. (2019). Design and suction performance test of sucking-seed plate combined with groove-tooth structure on high speed precision metering device of rapeseed (油菜高速精量排种器槽齿组合式吸种盘设计与吸附性能试验). *Transactions of the Chinese Society of Agricultural Engineering*, 35(1), 12-22. https://doi.org/10.11975/j.issn.1002-6819.2019.01.002

[17] Liu R., Liu Z., Zhao J., Lu Q., Liu L., & Li Y. (2022). Optimization and experiment of a disturbance-assisted seed filling high-speed vacuum seed-metering device based on DEM-CFD. *Agriculture*, 12(9), 1304. https://doi.org/10.3390/agriculture12091304

[18] Onal, I., Degirmencioglu, A., & Yazgi, A. (2012). An evaluation of seed spacing accuracy of a vacuum type precision metering unit based on theoretical considerations and experiments. *Turkish Journal of Agriculture and Forestry*, 36(2): 133-144. https://doi.org/10.3906/tar-1010-1316.

[19] Ren D., Liu Tao, Xia S., Chen Y., Wang W., & Li Z. (2024). Design and seed filling performance test of cavity plate combination hole type seeding plate for corn and soybean (玉米大豆兼用腔盘组合孔式排种盘设计与充种性能试验). *Transactions of the Chinese Society for Agricultural Machinery*, 55(2), 73-89. https://doi.org/10.6041/j.issn.1000-1298.2024.02.007

[20] Rezaei Asl A., Roudbari M., & Esmailzadeh E. (2019). Fabrication and evaluation of vacuumed metering drum performance for row planting of soybean with grease belt. *Agricultural Engineering International: CIGR Journal*, 21(4), 96-106.

[21] Shi S., Liu H., Wei G., Zhou J., Jian S., & Zhang R. (2020). Optimization and experiment of pneumatic seed metering device with guided assistant filling based on EDEM-CFD (基于 DEM-CFD 的驱导辅助充种气吸式排种器优化与试验). *Transactions of the Chinese Society for Agricultural Machinery*, 51(5), 54-66. https://doi.org/10.6041/j.issn.1000-1298.2020.05.006

[22] Singh R.C., Singh G., & Saraswat D.C. (2005). Optimisation of design and operational paramet ers of a pneumatic seed metering device for planting cottonseeds. *Biosystems Engineering*, 92 (4), 429-438. https://doi.org/10.1016/j.biosystemseng.2005.07.002

[23] Tan Y., Zhang Y., Jin Y., Liao Q., Li W., & Liao Y. (2025). Design and experiment of pneumatic -assisted seed collector for rapeseed and wheat. *Transactions of the CSAM*, 56(9), 105-116，18 7. https://doi.org/10.6041/j.issn.1000-1298.2025.09.009

[24] Wang B., Wang Z., Luo X., Zhang M., Fang L., Liu S., & Xu P. (2019). Design and experiment of wedge churning device for pneumatic cylinder-type seed metering device for hybrid rice (杂交稻气力滚筒集排式排种器楔形搅种装置设计与试验). *Transactions of the Chinese Society of Agricultural Engineering*, 35(23), 1-8. https://doi.org/10.11975/j.issn.1002-6819.2019.23.001

[25] Wang J., Sun W., Simionescu P. A., & Ju Y. (2023). Optimization of the fluted force-feed seede r meter with the helical roller using the discrete element method and response surface analysis. *Agriculture*, 13(7), 1400. https://doi.org/10.3390/agriculture13071400

[26] Wang Z., Hou Z., Bao L., Liu Y., Li B., & Guo F. (2025). Construction of ellipsoidal particle dis crete element model and calibration of simulation parameters. *INMATEH - Agricultural Engineering*. 77(3), https://doi.org/10.35633/inmateh-77-108

[27] Yazgi, A., & Degirmencioglu, A. (2007). Optimisation of the seed spacing uniformity performance of a vacuum-type precision seeder using response surface methodology. *Biosystems Engineering*, 97(3): 347-356. https://doi.org/10.1016/j.biosystemseng.2007.03.013.

[28] Yu D., Peng F., Zeng Z., Zhang M., Yang W., Zang Y., He J., Huang Y., Wu Y., Zhong W., Gu o Z., Liu J., Li G., Qin X., & Wang Z. (2024). Vibrational dynamics of rice precision hole seede rs and their impact on seed dispensation efficacy. *Agriculture*, 14(2), 324. https://doi.org/10.3390/agriculture14020324

[29] Zhang D., Huang Z., Chen Y., Yi S., & Li Y. (2025). Discrete element method based modeling and parameter calibration for millet threshing mixture. *Transactions of the CSAM*, 56(12), 354-36 5. https://doi.org/10.6041/j.issn.1000-1298.2025.12.032

[30] Zhang G., Zang Y., Luo X., Wang Z., Zhang Q., & Zhang S. (2015). Design and indoor simulat ed experiment of pneumatic rice seed metering device. *International Journal of Agricultural and Biological Engineering*, 8(4), 10–18. https://doi.org/10.3965/j.ijabe.20150804.162645